PROCEEDINGS OF SCIENCE

ONLINE ICRC 2021 THE ASTROPARTICLE PHYSICS CONFERENCE Berlin | Germany 37th International Cosmic Ray Conference 12–23 July 2021

Searching for Dark Matter from the Sun with the IceCube Detector

The IceCube Collaboration
(a complete list of authors can be found at the end of the proceedings)
E-mail: jlazar@icecube.wisc.edu

The existence of dark matter (DM) has been well-established by repeated experiments probing various length scales. Even though DM is expected to make up 85% of the current matter content of the Universe, its nature remains unknown. One broad class of corpuscular DM motivated by Standard Model (SM) extensions is weakly interacting massive particles (WIMPs). WIMPs can generically have a non-zero cross-section with SM nuclei, which allows them to scatter off nuclei in large celestial bodies such as the Sun, losing energy and becoming gravitationally bound in the process. After repeated scattering, WIMPs sink to the solar center, leading to an excess of WIMPs there. Subsequently, WIMPs can annihilate to stable SM particles, either directly or through a decay chain of unstable SM particles. Among stable SM particles, only neutrinos can escape the dense solar core. Thus, one may look for an excess of neutrinos from the Sun's direction as evidence of WIMPs. The IceCube Neutrino Observatory, which detects Cherenkov radiation of charged particles produced in neutrino interactions, is especially well-suited to such searches since it is sensitive to WIMPs with masses in the region preferred by supersymmetric extensions of the SM. In this contribution, I will present the results of IceCube's most recent solar WIMP search, which includes all neutrino flavors, covers the WIMP mass range from 10 GeV to 1 TeV, and has world-leading sensitivity over this entire range for most channels considered.

Corresponding authors: Jeffrey Lazar[1,2,*], Qinrui Liu[2], Carlos Argüelles[1], Ali Kheirandish[3]

[1] *Department of Physics and Laboratory for Particle Physics and Cosmology, Harvard University Cambridge, MA 02138, USA*
[2] *Dept. of Physics and Wisconsin IceCube Particle Astrophysics Center, University of Wisconsin–Madison Madison, WI 53706, USA*
[3] *Dept. of Astronomy and Astrophysics, Pennsylvania State University University Park, PA 16802, USA*

[*] Presenter

37th International Cosmic Ray Conference (ICRC 2021)
July 12th – 23rd, 2021
Online – Berlin, Germany

PoS(ICRC2021)020

1. Introduction

Astrophysical and cosmological observations provide strong evidence for the existence of dark matter (DM); however, the nature of DM remains unknown. One candidate class of DM is weakly interacting massive particles (WIMPs), which are expected to have masses from a few GeV to a few TeV; see [1] for a comprehensive review. Such particles can interact with Standard Model (SM) particles at or below the weak scale. These interactions allow for WIMPs to scatter off SM in large celestial bodies, losing energy in the process and possibly becoming gravitationally bound. While this can happen in any celestial body, in this work we will focus on capture by the Sun. Once captured, WIMPs will undergo additional scatterings, and fall to the center of the Sun [2, 3]. As WIMPs continue to be captured, an excess accumulates at the core of the Sun.

Another consequence of weakly interacting with the SM is that WIMPs can annihilate into SM particles [4]. This will create neutrinos, either as a primary product, or as a secondary product when unstable SM particle decay. One may then look for the neutrinos created by annihilating WIMPs as a DM signature. This approach to detecting DM is known as indirect detection. For WIMPs with mass above a few GeV, we expect the capture and annihilation processes to be in equilibrium in the Sun, *i.e.* the capture rate and annihlation rate are equal up to a factor of 2. For a given WIMP mass and solar model, the capture rate depends only on the WIMP-nucleon cross section, $\sigma_{\chi n}$ [5], one is able to probe the WIMP-nucleon cross section with solar WIMP searches.

To detect this flux, the IceCube Neutrino Observatory—a gigaton-scale neutrino telescope located in the ice beneath the South Pole—can look for an excess of neutrinos from the direction of the Sun. The size of the production region is smaller than the angular resolution of the IceCube observatory, and so this is essentially a point source with a time-variable source location. We expect the signal to be exponentially cut off above 3 TeV, since for neutrinos above this energy, the mean free path of the neutrino is less than the radius of the Sun. In this energy range, the only intrinsic background from the Sun are neutrinos produced in interactions between cosmic rays and the solar atmosphere. Additionally, we expect a background of neutrinos and muons from cosmic ray interactions in the Earth's atmosphere. The uncertainty in the intrinsic background is at the level of 30% [6–9], thus an observation of an excess above terrestrial and solar atmospheric backgrounds would be compelling evidence for new physics. This contrasts with other indirect searches, such as multimessenger detections from the galactic halo [10–14], where backgrounds are weakly constrained.

2. Signal

In order to compute the expected neutrino yield from WIMP annihilation in the Sun, one must must first compute the initial neutrino yield per annihilation in the center of the Sun. To do this, one must simulate interactions and decays of the primary SM products with the surrounding environment, and well as the interactions and decays of any secondary products which may be produced. This can then be propagated to the detector to compute the final neutrino yield.

We developed the χ`aro`ν software [15] in order to compute the neutrino yields from WIMP annihilation. This replaces `WimpSim` [16], which was used in the previous IceCube solar WIMP search. This software takes initial SM spectra from WIMP annihilation and recursively simulates

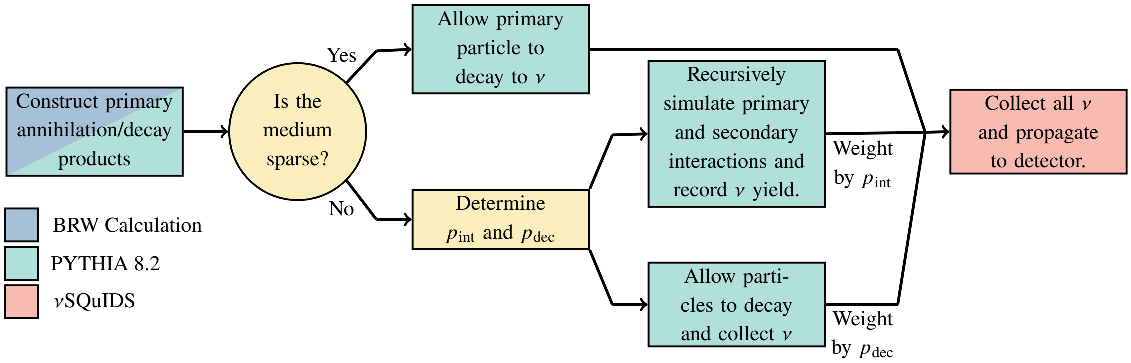

Figure 1: ***Flowchart of χarov algorithm.*** Flow chart depicting the major steps in the calculating flux from DM annihilation or decay. The light yellow boxes indicate direct calculation or decision making; other colors indicate the main program used in each step.

interaction and decay for the initial byproducts, and any secondary byproducts. Once all remaining particles are stable, it propagates the neutrinos from the center of the Sun to the detector using the νSQuIDS software; see Fig 1 for a visual representation of the algorithm. Natively, the initial SM spectrum from which the rest of the algorithm flows can be drawn from PYTHIA [17] or from a recent calculation of initial spectra by Bauer, Rodd, and Webber [18], henceforth called the BRW calculation.

The BRW calculation includes a full treatment of the electroweak (EW) correction, a phenomenon in which, high-energy particles can radiate weak gauge bosons in the same manner as photons may be radiated at lower energies. To do this, it evolves the initial spectrum from WIMP annihilation and evolves it from the WIMP scale using the DGLAP equations and matches it onto PYTHIA output in the regime in which PYTHIA has been well-validated by accelerator data. This improves on previous implementations of the EW correction, such as the Poor Particle Physicists Cookbook [19], which augmented PYTHIA with first order EW corrections, since it includes the full physics of the SM. This calculation can have dramatic effects on the initial spectra, hardening hadronic spectra since the radiated boson may give rise to a hard neutrino, and softening bosonic channels as the initial energy is split among the radiated bosons. See Fig. 2 for a comparison of initial ν_μ spectra from different signal simulations.

3. Backgrounds

3.1 Background Types

3.1.1 Atmospheric Muons

Atmospheric muons created in cosmic ray interactions can imitate the signal muons created from neutrinos that we are attempting to find. Such muons are the dominant source of background in the southern sky and taper off as the overburden increases in the northern sky. For this reason this analysis is mostly restricted events which seem to come from the northern sky. The Improved Northern Tracks selection is >99% pure in neutrinos, and so this background can safely be neglected.

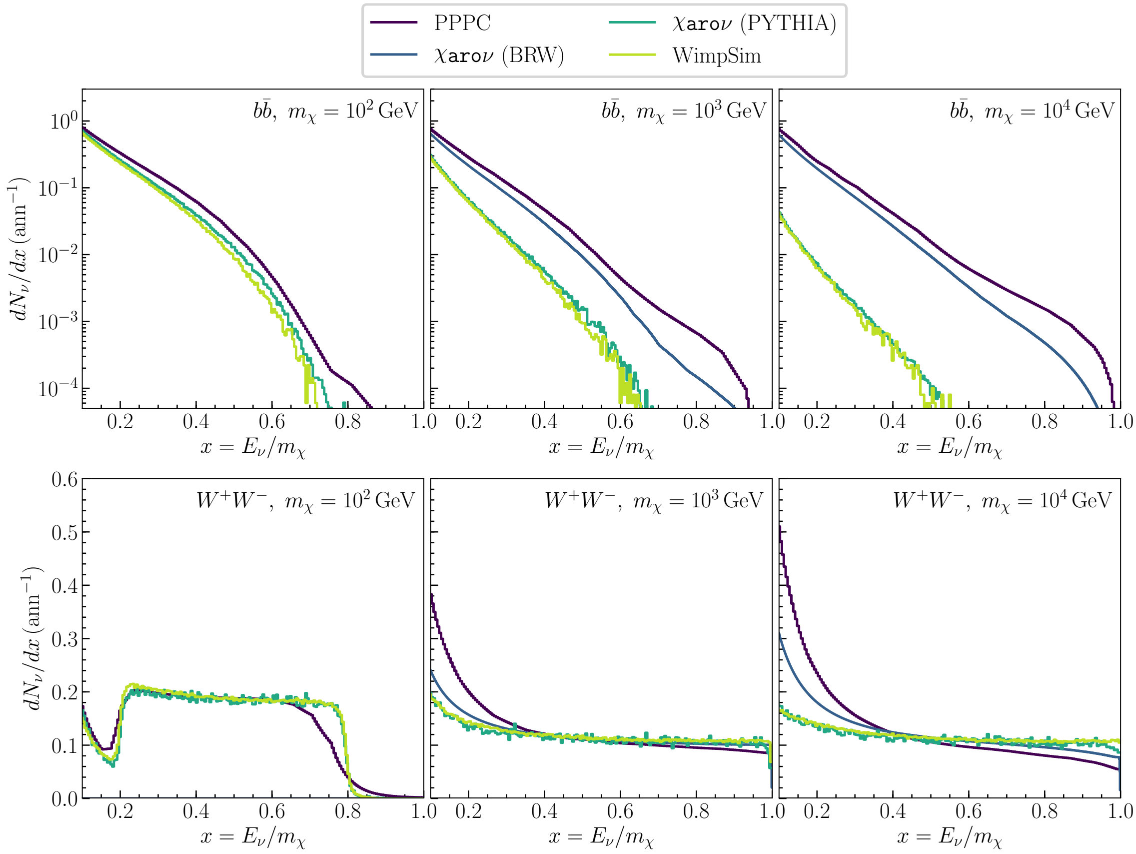

Figure 2: ***Comparison of ν_μ-yield using four different signal generators for DM at the Sun center.*** The major contribution to differences between the lines is that a more complete treatment of the EW correction has been implemented in PPPC and χaroν (BRW). As expected, the magnitude of this difference grows as the mass of the DM increases. When comparing the PYTHIA-based calculations, the $b\bar{b}$ channel in χaroν is slightly harder than WimpSim which is consistent with the result from [20]. The BRW calculation does not extend to masses below 500 GeV and so it is absent from the first column.

3.1.2 Atmospheric Neutrinos

The dominant background for this analysis is conventional atmospheric neutrinos, since these neutrinos can only be differentiated from the signal via the directional, flavor, and energy distribution. There are insufficient statistics to include these two latter pieces of information in the analysis, and so we must rely solely on the former.

3.1.3 Solar Atmospheric Neutrinos

There is small, well-predicted but yet unmeasured flux of neutrinos that comes from cosmic ray interactions with solar matter. Although small, this background also originates in the Sun, and so it cannot be differentiated by its directional distribution. This it is an irreducible background for this analysis. In fact the this flux creates a floor for solar WIMP searches as computed in [7, 8].

PoS(ICRC2021)020

3.2 Background from Data

We compute our background distributions from scrambled data. To do this, we sample random azimuth directions for each event. As long as an event is not near the polls, this will result in a randomized distribution while preserving the zenith dependence of the detector efficiency. This procedure will not work as well for events near the poles, *i.e.* $\cos\theta_{\text{zen}} \simeq \pm 1$; however, we do not need to worry about such events in this analysis since the Sun is never near the poles, and thus near-pole events will not contribute to the likelihood.

Computing our background in this way has a number of advantages, including freedom from systematic uncertainties associated with our background distributions. One challenge associated with this is that the limited data can lead to sparse expected background distributions. This issue is especially pronounced in the region of interest for this analysis, *i.e.* the few degrees around the Sun. The 5 degrees around the Sun only accounts for 0.2% of the phasespace, and so this region is particularly susceptible to erratic behavior associated with limited statistics.

To remedy this issue, we oversample the data, selecting many sets of random azimuth angles and dividing the total number of events by the number of sets generated. This preserves the number of events in the sample, but fills in gaps the distribution arising from limited statistics. See Fig. 3 for the expected distribution of background events in the 10 degrees surounding the Sun.

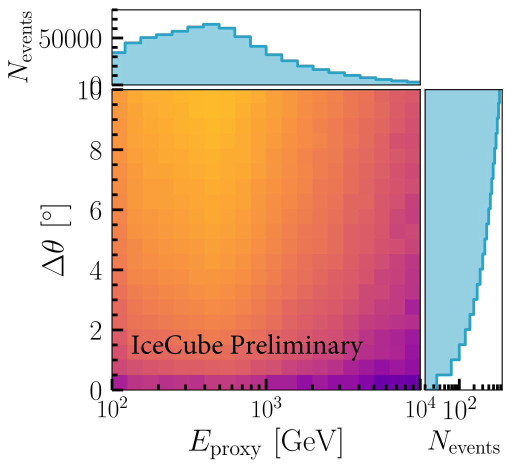

Figure 3: ***Background distribution from oversampled, scrambled data***. Distribution of background events in the region near the Sun as a function of the reconstructed energy and the opening angle from the center of the Sun. $N_{\text{events,bg}} = 665,291$

4. Event Selections

This analysis uses a custom event selection, combining preëxisting low- and high-energy selections with a medium-energy selection which is currently under development. This medium-energy selection is intended to bridge the gap between the low- and high-energy selection, see Fig. 4. The ~100 GeV region where this gap in coverage appears is particularly important for solar WIMP searches since it is the preferred region for the WIMP which occurs in supersymmetric extensions of the SM. All of these selections are so-called 'upgoing' selections, restricting themselves to regions where much of the atmospheric muon background has been filtered out by the Earth. The high-energy portion of the selection is a high-purity muon neutrino sample, while the low- and medium-energy selections contain all neutrino flavors. In this section, we will briefly outline the event selections being used for this analysis, and give current progress on the medium-energy selection.

4.1 Low-Energy Selection

Located within the IceCube instrumented volume is a more densely packed sub-detector known as DeepCore. In DeepCore, the inter-string distance ranges from 42 m to 72 m, while the vertical DOM spacing ranges from 7 m to 10 m. This higher density of DOMs allows DeepCore to detect neutrinos with energies as low as a few GeV.

OscNext is a suite of atmospheric neutrino oscillation analyses which use DeepCore data from 2011-2019. These analyses are joined by a common event selection whose purpose is to achieve a neutrino-dominated event sample by rejecting a prevailing background from atmospheric muons and detector noise. While, this event selection is quite sophisticated and describing it thoroughly is beyond the scope of this proceeding, we will outline a few aspects of the selection which will be important later. We do encourage the reader to read more detailed descriptions of the selection

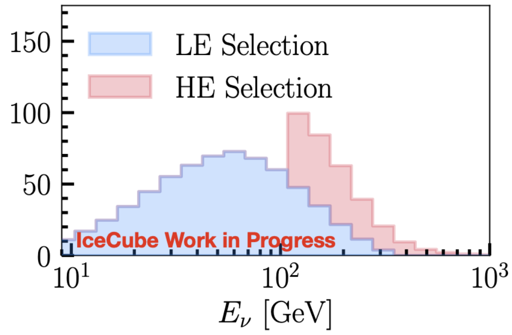

Figure 4: ***Stacked distribution solar WIMP rates.*** Rates for $\chi\chi \rightarrow b\bar{b}$ with $m_\chi = 500$ GeV as a function of true neutrino energy in the low-energy (blue) and high-energy (red) selections. Note the gap in coverage for neutrinos with energies in the range of 80 GeV to 300 GeV. y-axis in arbitrary units

The final selection contains neutrinos with reconstructed energies ranging from 5 GeV to 300 GeV, and contains all neutrino flavors. At final level, the sample has a nominal neutrino rate of 0.991 mHz, a nominal muon rate of 0.034 mHz, and a nominal noise rate of 0.000 mHz. The selection obtains this level of purity using a series of selection cuts combining traditional straight cuts and boosted decision trees (BDTs). Additionally, oscNext uses a BDT to differentiate between cascades and tracks. This approach of successive BDTs will be emulated in the medium event selection as well.

For Analysis B, we use a modified version of the oscNext selection. The first modification is to remove events which overlap with the high-energy selection. This ensuers that events are not being double counted and that the selections are statistically independent. Furthermore, we are investigating the effect of relaxing oscNext cuts on our sensitivity. Since this analysis amounts to looking for a point source, we may be able to tolerate more background than the oscNext analyses.

4.2 High-energy Selection

For high energy events, we use a newer IceCube dataset using 9 years of 86-string data from 2011 to 2020, notably including the solar minimum of 2019-2020. This newer IceCube dataset features an improved energy reconstruction and angular reconstruction, and includes data from all 9 years feature the full detector configuration. The event selection is limited to upgoing events, using the Earth as an effective atmospheric muon veto to create a high-purity neutrino sample. The event selection is limited to $\nu_\mu + \bar{\nu}_\mu$ events, owing to their superior angular reconstruction at high-energies. Compared to the OscNext selection, this leads to events being more concentrated in the direction of the sun.

4.3 Medium Energy Selection

At around E_ν =100 GeV, there is a gap in coverage between the low- and high-energy selections, see Fig. 4. Since the flux of solar atmospheric neutrinos is higher at lower energies, it is import to have coverage in this energy regime. To do this, we employ IceCube's 'LowUp Filter.' This low-level trigger was designed to target low-energy, up-going neutrinos. This was originally used in IceCube's searches for neutrinos coming from dark matter annihilation in the Sun. In such analyses, the 100 GeV region is important for theoretical reasons. Since these analyses share a source origin and target energy regime, it is natural to adapt the methods of one to the other.

After having selected events which pass the LowUp filter and having filtered events which may be in other portions of the selection, we plan to emulate the approach of the low-energy selection. We perform computationally inexpensive reconstructions and make a conservative cut on zenith angle to filter out much of the atmospheric muon background which dominates in the southern sky. After this cut, the data rate is sufficiently low to use a BDT to differentiate muons from neutrinos; see Fig. 5 for the current performance of this BDT. At this point, the data rate has been cut to a sufficiently low level to allow more computationally expensive reconstructions to be run. We are in the process of studying different reconstructions in order to understand which will optimize our sensitivity.

Finally, we intend to make a final BDT to differentiate solar atmospheric neutrinos from conventional atmospheric neutrinos. While this is difficult given that both are neutrinos, there are differences between the two populations. First, there are differences in the zenith and energy spectra of the two populations. Additionally, while the flavor composition of each is the same at production, solar atmospheric neutrinos are able to oscillate into other flavors, leading to more cascade-like events in the solar atmospheric population. To exploit this latter fact, we will include metrics which are tied to particle identification in this BDT, in addition to directional and energy quantities. Since the result of this BDT is unlikely to provide clear distinction between the two populations, we plan to let the output of it enter as an analysis variable.

5. Analysis Methods

5.1 Binned Likelihood Analysis

The second analysis uses a binned likelihood method. Since each portion of the event selection is independent by construction, the likelihood factors to give:

$$\mathcal{L}_{\text{tot}} = \mathcal{L}_{\text{LE}}\,\mathcal{L}_{\text{ME}}\,\mathcal{L}_{\text{HE}}, \tag{1}$$

where $\mathcal{L}_{\text{LE}}$, $\mathcal{L}_{\text{ME}}$, and $\mathcal{L}_{\text{HE}}$ are the likelihoods for the low-energy, medium-energy, and high-energy subselections. In the i^{th} bin, given a nominal number signal events $\mu_{s,i}$ and nominal number of background events $\mu_{s,i}$, we define the likelihood as:

$$\mathcal{L}(n_s, n_b|\mu_{s,i}, \mu_{b,i}) = \frac{e^{-\mu_i} \cdot \mu_i^{\mu_{b,i}}}{\mu_{b,i}!}, \tag{2}$$

where n_s and n_b are the normalizations of the signal and background distributions with respect to the nominal models and $\mu_i = n_s\mu_{s,i} + n_b\mu_{b,i}$. We then define the contribution of the i^{th} to the test

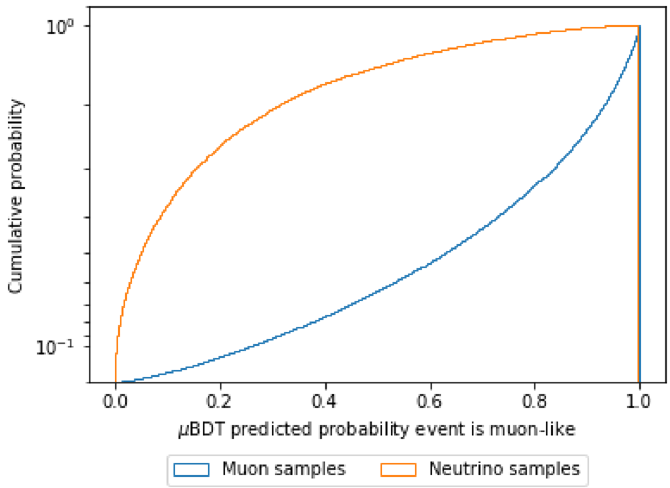

Figure 5: ***Performance of the μBDT.*** Initial performance of the BDT which will be used to differentiate muons from neutrinos. By retaining only events with a score lower than 0.25, we can retain 90% of neutrino events while cutting the muon background by an order of magnitude.

statistic of a model hypothesis as:

$$TS_i = TS(n_s, n_b|\mu_{s,i}, \mu_{b,i}) = -2\log\left(\frac{\mathcal{L}(n_s, n_b|\mu_{s,i}, \mu_{b,i})}{\mathcal{L}(0, n_b|\mu_{s,i}, \mu_{b,i})}\right). \tag{3}$$

The total test statistic is given by a double sum over the bins in each subselction and over the subselections themselves, *i.e.*:

$$TS = -2\sum_{j}^{\{\text{LE,ME,HE}\}}\sum_{i}\log\left(\frac{\mathcal{L}_j(n_s, n_b|\mu_{s,i}, \mu_{b,i})}{\mathcal{L}_j(0, n_b|\mu_{s,i}, \mu_{b,i})}\right) \tag{4}$$

We may then compute our sensitivity to a given model by randomly choosing numbers from a Poisson distribution with an expectation in each bin equal to $n_s\mu_{s,i} + \mu_b$

6. Results

In Fig 6, we show sensitivities computed using the low- and high-energy portion of this event selection, compared to limits obtained from previous solar WIMP analyses. This analysis has world-leading sensitivities over the WIMP mass range from $m_\chi = 10$ GeV to $m_\chi = 10$ TeV under the assumption that WIMPs annihilate to the W^+W^- or $\tau^+\tau^-$. Under the assumtion that WIMPs annihilate to $b\bar{b}$, Super-Kamiokande is more sensitive for $m_\chi = 10$ GeV. This is because hadronic channels are generically softer, and so Super-Kamiokande, which is optimized for lower-energy neutrinos, has an advantage in this channel.

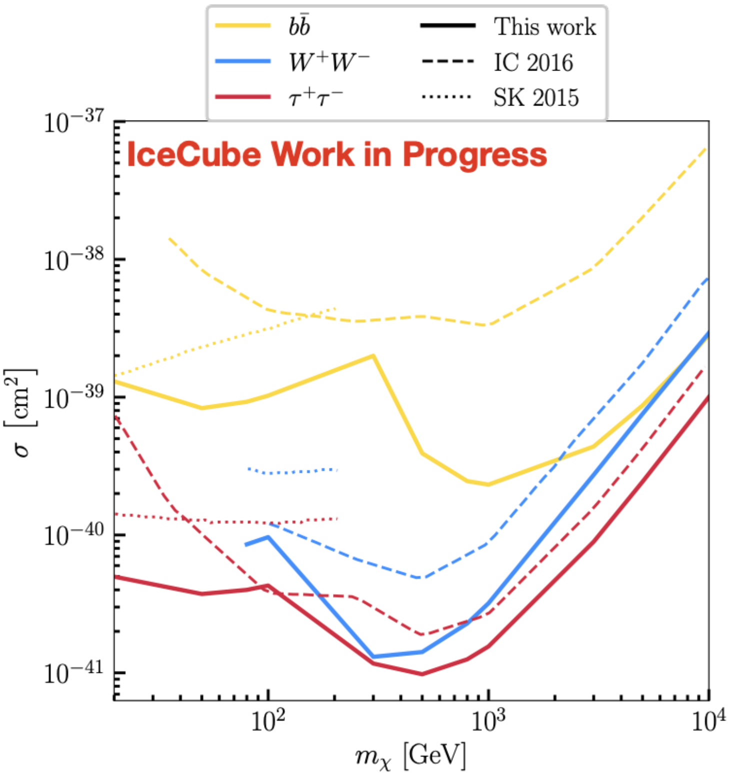

Figure 6: ***Sensitivities of this analysis using low- and high-energy selection.***

References

[1] G. Bertone, D. Hooper and J. Silk, *Particle dark matter: Evidence, candidates and constraints*, *Phys. Rept.* **405** (2005) 279 [hep-ph/0404175].

[2] S. Ritz and D. Seckel, *Detailed Neutrino Spectra From Cold Dark Matter Annihilations in the Sun*, *Nucl. Phys.* **B304** (1988) 877.

[3] M. Srednicki, K.A. Olive and J. Silk, *High-Energy Neutrinos from the Sun and Cold Dark Matter*, *Nucl. Phys.* **B279** (1987) 804.

[4] T.K. Gaisser, G. Steigman and S. Tilav, *Limits on Cold Dark Matter Candidates from Deep Underground Detectors*, *Phys. Rev. D* **34** (1986) 2206.

[5] A. Gould, *Cosmological density of WIMPs from solar and terrestrial annihilations*, *Astrophys. J.* **388** (1992) 338.

[6] G. Ingelman and M. Thunman, *High-energy neutrino production by cosmic ray interactions in the sun*, *Phys. Rev. D* **54** (1996) 4385 [hep-ph/9604288].

[7] C.A. Argüelles, G. de Wasseige, A. Fedynitch and B.J.P. Jones, *Solar Atmospheric Neutrinos and the Sensitivity Floor for Solar Dark Matter Annihilation Searches*, *JCAP* **07** (2017) 024 [1703.07798].

[8] K.C.Y. Ng, J.F. Beacom, A.H.G. Peter and C. Rott, *Solar Atmospheric Neutrinos: A New Neutrino Floor for Dark Matter Searches*, *Phys. Rev. D* **96** (2017) 103006 [1703.10280].

[9] J. Edsjö, J. Elevant, R. Enberg and C. Niblaeus, *Neutrinos from cosmic ray interactions in the sun*, *Journal of Cosmology and Astroparticle Physics* **2017** (2017) 033–033.

[10] IceCube collaboration, *Multipole analysis of IceCube data to search for dark matter accumulated in the Galactic halo*, *Eur. Phys. J. C* **75** (2015) 20 [1406.6868].

[11] IceCube collaboration, *Search for Dark Matter Annihilation in the Galactic Center with IceCube-79*, *Eur. Phys. J. C* **75** (2015) 492 [1505.07259].

[12] HAWC collaboration, *A Search for Dark Matter in the Galactic Halo with HAWC*, *JCAP* **02** (2018) 049 [1710.10288].

[13] ANTARES collaboration, *Search for dark matter towards the Galactic Centre with 11 years of ANTARES data*, *Phys. Lett. B* **805** (2020) 135439 [1912.05296].

[14] ANTARES, IceCube collaboration, *Combined search for neutrinos from dark matter self-annihilation in the Galactic Center with ANTARES and IceCube*, *Phys. Rev. D* **102** (2020) 082002 [2003.06614].

[15] Q. Liu, J. Lazar, C.A. Argüelles and A. Kheirandish, *χarov: a tool for neutrino flux generation from WIMPs*, *JCAP* **10** (2020) 043 [2007.15010].

[16] M. Blennow, J. Edsjö and T. Ohlsson, *Neutrinos from WIMP annihilations using a full three-flavor Monte Carlo*, *JCAP* **0801** (2008) 021 [0709.3898].

[17] T. Sjöstrand, S. Ask, J.R. Christiansen, R. Corke, N. Desai, P. Ilten et al., *An introduction to PYTHIA 8.2*, *Comput. Phys. Commun.* **191** (2015) 159 [1410.3012].

[18] C.W. Bauer, N.L. Rodd and B.R. Webber, *Dark Matter Spectra from the Electroweak to the Planck Scale*, 2007.15001.

[19] P. Baratella, M. Cirelli, A. Hektor, J. Pata, M. Piibeleht and A. Strumia, *PPPC 4 DMν: a Poor Particle Physicist Cookbook for Neutrinos from Dark Matter annihilations in the Sun*, *JCAP* **1403** (2014) 053 [1312.6408].

[20] M. Cirelli, N. Fornengo, T. Montaruli, I.A. Sokalski, A. Strumia and F. Vissani, *Spectra of neutrinos from dark matter annihilations*, *Nucl. Phys.* **B727** (2005) 99 [hep-ph/0506298].

Full Author List: IceCube Collaboration

R. Abbasi[17], M. Ackermann[59], J. Adams[18], J. A. Aguilar[12], M. Ahlers[22], M. Ahrens[50], C. Alispach[28], A. A. Alves Jr.[31], N. M. Amin[42], R. An[14], K. Andeen[40], T. Anderson[56], G. Anton[26], C. Argüelles[14], Y. Ashida[38], S. Axani[15], X. Bai[46], A. Balagopal V.[38], A. Barbano[28], S. W. Barwick[30], B. Bastian[59], V. Basu[38], S. Baur[12], R. Bay[8], J. J. Beatty[20, 21], K.-H. Becker[58], J. Becker Tjus[11], C. Bellenghi[27], S. BenZvi[48], D. Berley[19], E. Bernardini[59, 60], D. Z. Besson[34, 61], G. Binder[8, 9], D. Bindig[58], E. Blaufuss[19], S. Blot[59], M. Boddenberg[1], F. Bontempo[31], J. Borowka[1], S. Böser[39], O. Botner[57], J. Böttcher[1], E. Bourbeau[22], F. Bradascio[59], J. Braun[38], S. Bron[28], J. Brostean-Kaiser[59], S. Browne[32], A. Burgman[57], R. T. Burley[2], R. S. Busse[41], M. A. Campana[45], E. G. Carnie-Bronca[2], C. Chen[6], D. Chirkin[38], K. Choi[52], B. A. Clark[24], K. Clark[33], L. Classen[41], A. Coleman[42], G. H. Collin[15], J. M. Conrad[15], P. Coppin[13], P. Correa[13], D. F. Cowen[55, 56], R. Cross[48], C. Dappen[1], P. Dave[6], C. De Clercq[13], J. J. DeLaunay[56], H. Dembinski[42], K. Deoskar[50], S. De Ridder[29], A. Desai[38], P. Desiati[38], K. D. de Vries[13], G. de Wasseige[13], M. de With[10], T. DeYoung[24], S. Dharani[1], A. Diaz[15], J. C. Díaz-Vélez[38], M. Dittmer[41], H. Dujmovic[31], M. Dunkman[56], M. A. DuVernois[38], E. Dvorak[46], T. Ehrhardt[39], P. Eller[27], R. Engel[31, 32], H. Erpenbeck[1], J. Evans[19], P. A. Evenson[42], K. L. Fan[19], A. R. Fazely[7], S. Fiedlschuster[26], A. T. Fienberg[56], K. Filimonov[8], C. Finley[50], L. Fischer[59], D. Fox[55], A. Franckowiak[11, 59], E. Friedman[19], A. Fritz[39], P. Fürst[1], T. K. Gaisser[42], J. Gallagher[37], E. Ganster[1], A. Garcia[14], S. Garrappa[59], L. Gerhardt[9], A. Ghadimi[54], C. Glaser[57], T. Glauch[27], T. Glüsenkamp[26], A. Goldschmidt[9], J. G. Gonzalez[42], S. Goswami[54], D. Grant[24], T. Grégoire[56], S. Griswold[48], M. Gündüz[11], C. Günther[1], C. Haack[27], A. Hallgren[57], R. Halliday[24], L. Halve[1], F. Halzen[38], M. Ha Minh[27], K. Hanson[38], J. Hardin[38], A. A. Harnisch[24], A. Haungs[31], S. Hauser[1], D. Hebecker[10], K. Helbing[58], F. Henningsen[27], E. C. Hettinger[24], S. Hickford[58], J. Hignight[25], C. Hill[16], G. C. Hill[2], K. D. Hoffman[19], R. Hoffmann[58], T. Hoinka[23], B. Hokanson-Fasig[38], K. Hoshina[38, 62], F. Huang[56], M. Huber[27], T. Huber[31], K. Hultqvist[50], M. Hünnefeld[23], R. Hussain[38], S. In[52], N. Iovine[12], A. Ishihara[16], M. Jansson[50], G. S. Japaridze[5], M. Jeong[52], B. J. P. Jones[4], D. Kang[31], W. Kang[52], X. Kang[45], A. Kappes[41], D. Kappesser[39], T. Karg[59], M. Karl[27], A. Karle[38], U. Katz[26], M. Kauer[38], M. Kellermann[1], J. L. Kelley[38], A. Kheirandish[56], K. Kin[16], T. Kintscher[59], J. Kiryluk[51], S. R. Klein[8, 9], R. Koirala[42], H. Kolanoski[10], T. Kontrimas[27], L. Köpke[39], C. Kopper[24], S. Kopper[54], D. J. Koskinen[22], P. Koundal[31], M. Kovacevich[45], M. Kowalski[10, 59], T. Kozynets[22], E. Kun[11], N. Kurahashi[45], N. Lad[59], C. Lagunas Gualda[59], J. L. Lanfranchi[56], M. J. Larson[19], F. Lauber[58], J. P. Lazar[14, 38], J. W. Lee[52], K. Leonard[38], A. Leszczyńska[32], Y. Li[56], M. Lincetto[11], Q. R. Liu[38], M. Liubarska[25], E. Lohfink[39], C. J. Lozano Mariscal[41], L. Lu[38], F. Lucarelli[28], A. Ludwig[24, 35], W. Luszczak[38], Y. Lyu[8, 9], W. Y. Ma[59], J. Madsen[38], K. B. M. Mahn[24], Y. Makino[38], S. Mancina[38], I. C. Mariş[12], R. Maruyama[43], K. Mase[16], T. McElroy[25], F. McNally[36], J. V. Mead[22], K. Meagher[38], A. Medina[21], M. Meier[16], S. Meighen-Berger[27], J. Micallef[24], D. Mockler[12], T. Montaruli[28], R. W. Moore[25], R. Morse[38], M. Moulai[15], R. Naab[59], R. Nagai[16], U. Naumann[58], J. Necker[59], L. V. Nguyễn[24], H. Niederhausen[27], M. U. Nisa[24], S. C. Nowicki[24], D. R. Nygren[9], A. Obertacke Pollmann[58], M. Oehler[31], A. Olivas[19], E. O'Sullivan[57], H. Pandya[42], D. V. Pankova[56], N. Park[33], G. K. Parker[4], E. N. Paudel[42], L. Paul[40], C. Pérez de los Heros[57], L. Peters[1], J. Peterson[38], S. Philippen[1], D. Pieloth[23], S. Pieper[58], M. Pittermann[32], A. Pizzuto[38], M. Plum[40], Y. Popovych[39], A. Porcelli[29], M. Prado Rodriguez[38], P. B. Price[8], B. Pries[24], G. T. Przybylski[9], C. Raab[12], A. Raissi[18], M. Rameez[22], K. Rawlins[3], I. C. Rea[27], A. Rehman[42], P. Reichherzer[11], R. Reimann[1], G. Renzi[12], E. Resconi[27], S. Reusch[59], W. Rhode[23], M. Richman[45], B. Riedel[38], E. J. Roberts[2], S. Robertson[8, 9], G. Roellinghoff[52], M. Rongen[39], C. Rott[49, 52], T. Ruhe[23], D. Ryckbosch[29], D. Rysewyk Cantu[24], I. Safa[14, 38], J. Saffer[32], S. E. Sanchez Herrera[24], A. Sandrock[23], J. Sandroos[39], M. Santander[54], S. Sarkar[44], S. Sarkar[25], K. Satalecka[59], M. Scharf[1], M. Schaufel[1], H. Schieler[31], S. Schindler[26], P. Schlunder[23], T. Schmidt[19], A. Schneider[38], J. Schneider[26], F. G. Schröder[31, 42], L. Schumacher[27], G. Schwefer[1], S. Sclafani[45], D. Seckel[42], S. Seunarine[47], A. Sharma[57], S. Shefali[32], M. Silva[38], B. Skrzypek[14], B. Smithers[4], R. Snihur[38], J. Soedingrekso[23], D. Soldin[42], C. Spannfellner[27], G. M. Spiczak[47], C. Spiering[59, 61], J. Stachurska[59], M. Stamatikos[21], T. Stanev[42], R. Stein[59], J. Stettner[1], A. Steuer[39], T. Stezelberger[9], T. Stürwald[58], T. Stuttard[22], G. W. Sullivan[19], I. Taboada[6], F. Tenholt[11], S. Ter-Antonyan[7], S. Tilav[42], F. Tischbein[1], K. Tollefson[24], L. Tomankova[11], C. Tönnis[53], S. Toscano[12], D. Tosi[38], A. Trettin[59], M. Tselengidou[26], C. F. Tung[6], A. Turcati[27], R. Turcotte[31], C. F. Turley[56], J. P. Twagirayezu[24], B. Ty[38], M. A. Unland Elorrieta[41], N. Valtonen-Mattila[57], J. Vandenbroucke[38], N. van Eijndhoven[13], D. Vannerom[15], J. van Santen[59], S. Verpoest[29], M. Vraeghe[29], C. Walck[50], T. B. Watson[4], C. Weaver[24], P. Weigel[15], A. Weindl[31], M. J. Weiss[56], J. Weldert[39], C. Wendt[38], J. Werthebach[23], M. Weyrauch[32], N. Whitehorn[24, 35], C. H. Wiebusch[1], D. R. Williams[54], M. Wolf[27], K. Woschnagg[8], G. Wrede[26], J. Wulff[11], X. W. Xu[7], Y. Xu[51], J. P. Yanez[25], S. Yoshida[16], S. Yu[24], T. Yuan[38], Z. Zhang[51]

[1] III. Physikalisches Institut, RWTH Aachen University, D-52056 Aachen, Germany
[2] Department of Physics, University of Adelaide, Adelaide, 5005, Australia
[3] Dept. of Physics and Astronomy, University of Alaska Anchorage, 3211 Providence Dr., Anchorage, AK 99508, USA
[4] Dept. of Physics, University of Texas at Arlington, 502 Yates St., Science Hall Rm 108, Box 19059, Arlington, TX 76019, USA
[5] CTSPS, Clark-Atlanta University, Atlanta, GA 30314, USA
[6] School of Physics and Center for Relativistic Astrophysics, Georgia Institute of Technology, Atlanta, GA 30332, USA
[7] Dept. of Physics, Southern University, Baton Rouge, LA 70813, USA
[8] Dept. of Physics, University of California, Berkeley, CA 94720, USA
[9] Lawrence Berkeley National Laboratory, Berkeley, CA 94720, USA
[10] Institut für Physik, Humboldt-Universität zu Berlin, D-12489 Berlin, Germany
[11] Fakultät für Physik & Astronomie, Ruhr-Universität Bochum, D-44780 Bochum, Germany
[12] Université Libre de Bruxelles, Science Faculty CP230, B-1050 Brussels, Belgium
[13] Vrije Universiteit Brussel (VUB), Dienst ELEM, B-1050 Brussels, Belgium
[14] Department of Physics and Laboratory for Particle Physics and Cosmology, Harvard University, Cambridge, MA 02138, USA
[15] Dept. of Physics, Massachusetts Institute of Technology, Cambridge, MA 02139, USA

[16] Dept. of Physics and Institute for Global Prominent Research, Chiba University, Chiba 263-8522, Japan
[17] Department of Physics, Loyola University Chicago, Chicago, IL 60660, USA
[18] Dept. of Physics and Astronomy, University of Canterbury, Private Bag 4800, Christchurch, New Zealand
[19] Dept. of Physics, University of Maryland, College Park, MD 20742, USA
[20] Dept. of Astronomy, Ohio State University, Columbus, OH 43210, USA
[21] Dept. of Physics and Center for Cosmology and Astro-Particle Physics, Ohio State University, Columbus, OH 43210, USA
[22] Niels Bohr Institute, University of Copenhagen, DK-2100 Copenhagen, Denmark
[23] Dept. of Physics, TU Dortmund University, D-44221 Dortmund, Germany
[24] Dept. of Physics and Astronomy, Michigan State University, East Lansing, MI 48824, USA
[25] Dept. of Physics, University of Alberta, Edmonton, Alberta, Canada T6G 2E1
[26] Erlangen Centre for Astroparticle Physics, Friedrich-Alexander-Universität Erlangen-Nürnberg, D-91058 Erlangen, Germany
[27] Physik-department, Technische Universität München, D-85748 Garching, Germany
[28] Département de physique nucléaire et corpusculaire, Université de Genève, CH-1211 Genève, Switzerland
[29] Dept. of Physics and Astronomy, University of Gent, B-9000 Gent, Belgium
[30] Dept. of Physics and Astronomy, University of California, Irvine, CA 92697, USA
[31] Karlsruhe Institute of Technology, Institute for Astroparticle Physics, D-76021 Karlsruhe, Germany
[32] Karlsruhe Institute of Technology, Institute of Experimental Particle Physics, D-76021 Karlsruhe, Germany
[33] Dept. of Physics, Engineering Physics, and Astronomy, Queen's University, Kingston, ON K7L 3N6, Canada
[34] Dept. of Physics and Astronomy, University of Kansas, Lawrence, KS 66045, USA
[35] Department of Physics and Astronomy, UCLA, Los Angeles, CA 90095, USA
[36] Department of Physics, Mercer University, Macon, GA 31207-0001, USA
[37] Dept. of Astronomy, University of Wisconsin–Madison, Madison, WI 53706, USA
[38] Dept. of Physics and Wisconsin IceCube Particle Astrophysics Center, University of Wisconsin–Madison, Madison, WI 53706, USA
[39] Institute of Physics, University of Mainz, Staudinger Weg 7, D-55099 Mainz, Germany
[40] Department of Physics, Marquette University, Milwaukee, WI, 53201, USA
[41] Institut für Kernphysik, Westfälische Wilhelms-Universität Münster, D-48149 Münster, Germany
[42] Bartol Research Institute and Dept. of Physics and Astronomy, University of Delaware, Newark, DE 19716, USA
[43] Dept. of Physics, Yale University, New Haven, CT 06520, USA
[44] Dept. of Physics, University of Oxford, Parks Road, Oxford OX1 3PU, UK
[45] Dept. of Physics, Drexel University, 3141 Chestnut Street, Philadelphia, PA 19104, USA
[46] Physics Department, South Dakota School of Mines and Technology, Rapid City, SD 57701, USA
[47] Dept. of Physics, University of Wisconsin, River Falls, WI 54022, USA
[48] Dept. of Physics and Astronomy, University of Rochester, Rochester, NY 14627, USA
[49] Department of Physics and Astronomy, University of Utah, Salt Lake City, UT 84112, USA
[50] Oskar Klein Centre and Dept. of Physics, Stockholm University, SE-10691 Stockholm, Sweden
[51] Dept. of Physics and Astronomy, Stony Brook University, Stony Brook, NY 11794-3800, USA
[52] Dept. of Physics, Sungkyunkwan University, Suwon 16419, Korea
[53] Institute of Basic Science, Sungkyunkwan University, Suwon 16419, Korea
[54] Dept. of Physics and Astronomy, University of Alabama, Tuscaloosa, AL 35487, USA
[55] Dept. of Astronomy and Astrophysics, Pennsylvania State University, University Park, PA 16802, USA
[56] Dept. of Physics, Pennsylvania State University, University Park, PA 16802, USA
[57] Dept. of Physics and Astronomy, Uppsala University, Box 516, S-75120 Uppsala, Sweden
[58] Dept. of Physics, University of Wuppertal, D-42119 Wuppertal, Germany
[59] DESY, D-15738 Zeuthen, Germany
[60] Università di Padova, I-35131 Padova, Italy
[61] National Research Nuclear University, Moscow Engineering Physics Institute (MEPhI), Moscow 115409, Russia
[62] Earthquake Research Institute, University of Tokyo, Bunkyo, Tokyo 113-0032, Japan

Acknowledgements

USA – U.S. National Science Foundation-Office of Polar Programs, U.S. National Science Foundation-Physics Division, U.S. National Science Foundation-EPSCoR, Wisconsin Alumni Research Foundation, Center for High Throughput Computing (CHTC) at the University of Wisconsin–Madison, Open Science Grid (OSG), Extreme Science and Engineering Discovery Environment (XSEDE), Frontera computing project at the Texas Advanced Computing Center, U.S. Department of Energy-National Energy Research Scientific Computing Center, Particle astrophysics research computing center at the University of Maryland, Institute for Cyber-Enabled Research at Michigan State University, and Astroparticle physics computational facility at Marquette University; Belgium – Funds for Scientific Research (FRS-FNRS and FWO), FWO Odysseus and Big Science programmes, and Belgian Federal Science Policy Office (Belspo); Germany – Bundesministerium für Bildung und Forschung (BMBF), Deutsche Forschungsgemeinschaft (DFG), Helmholtz Alliance for Astroparticle Physics (HAP), Initiative and Networking Fund of the Helmholtz Association, Deutsches Elektronen Synchrotron (DESY), and High Performance Computing cluster of the RWTH Aachen; Sweden – Swedish Research Council, Swedish Polar Research Secretariat, Swedish National Infrastructure for Computing (SNIC), and Knut and Alice Wallenberg Foundation; Australia – Australian

Research Council; Canada – Natural Sciences and Engineering Research Council of Canada, Calcul Québec, Compute Ontario, Canada Foundation for Innovation, WestGrid, and Compute Canada; Denmark – Villum Fonden and Carlsberg Foundation; New Zealand – Marsden Fund; Japan – Japan Society for Promotion of Science (JSPS) and Institute for Global Prominent Research (IGPR) of Chiba University; Korea – National Research Foundation of Korea (NRF); Switzerland – Swiss National Science Foundation (SNSF); United Kingdom – Department of Physics, University of Oxford.